


Cite this: *RSC Adv.*, 2021, 11, 35311

# Microflowers formed by complexation-driven self-assembly between palladium(II) and bis-theophyllines: immortal catalyst for C–C cross-coupling reactions†

Katsuya Kaikake,<sup>ID\*</sup> Naoki Jou, Go Shitara and Ren-Hua Jin<sup>ID\*</sup>

The Pd catalyst for Suzuki–Miyaura or the other C–C coupling reactions is one of the central tools in organic synthesis related to medicine, agricultural chemicals and advanced materials. However, recycling palladium is a bottleneck for developing the extreme potential of Pd in chemistry. Herein, we established a new heterogeneous Pd catalytic system in which the catalyst is a nanopetal-gathered flower-like microsphere self-assembled from PdCl<sub>2</sub> and alkyl-linked bis-theophyllines. The microflowers catalyzed quantitatively the reaction of aryl bromides and phenylboronic acid in aqueous media at room temperature. It was found that the reaction proceeds better in an air atmosphere than in nitrogen gas even though the Pd(II) species employed was lowered to 0.001 mol% in the substance. Very interestingly, the microflowers could be recycled 20 times without deactivation in the C–C coupling reaction between bromobenzene and phenylboronic acid in the presence of sodium chloride. We found that the sodium chloride added played an important role in maintaining the morphology of microflowers and preventing the formation of metallic Pd particles.

Received 16th August 2021  
Accepted 25th October 2021

DOI: 10.1039/d1ra06177a

rsc.li/rsc-advances

## Introduction

The Suzuki–Miyaura cross-coupling reaction catalyzed by palladium complexes is widely employed as an extremely useful and central tool for the synthesis of pharmaceuticals, fine chemicals and materials of electronic devices such as OLEDs.<sup>1–6</sup> Therefore, great efforts have been invested in the development of palladium catalysts from the view of both homogeneous and heterogeneous architecture. In the homogeneous system, a lot of excellent palladium catalysts have been explored from the findings of structurally defined catalysts of palladacycles with phosphine ligands by Herrmann and Beller *et al.*<sup>7,8</sup> In particular, Buchwald pre-catalysis with up-dated generation exhibited remarkable progress in which a combination of various pre-catalysts with paradacycles and secondary phosphines greatly enhanced not only the catalysis efficiency but also the stability under air conditions. In Buchwald catalysts, the important feature is to activate oxidative addition by altering the electron donating group and to promote reductive elimination by introduction of bulky substituents surrounding the palladium center.<sup>9–12</sup> Although the up-dated generations of Buchwald catalysis resolved many disadvantages of conventional

palladium catalysts and have been commercialized as different generations, they are always limited in homogeneous state.

In parallel, the use of heterogeneous palladium catalysts in the C–C coupling reaction has been extensively studied from the viewpoint of reducing the contamination of palladium into products and reusing expensive catalysts.<sup>13–15</sup> Various heterogeneous palladium catalysts, such as self-assembled supramolecules and polymers, nanoparticles, MOF, ionic liquid, and carbon and silica support, have been developed. Among them, palladium nanoparticles with small size, rich surface area and defined morphologies could exhibit high catalytic activity, stability and selectivity.<sup>16–20</sup> It was reported that the catalytic activity of Pd-nanoparticles is arisen from a vertex and/or edge atom on crystalline Pd-nanoparticles that play as an active site.<sup>21–23</sup> Robust MOF with a uniform distribution of Pd shows excellent stability in air and high catalytic activity in Suzuki–Miyaura reaction, and thus Pd-MOF showed good performance in recyclability with easy-handing separation.<sup>24–26</sup> N-heterocyclic carbene (NHC) complexes like imidazolium-based complexes have strong sigma donor capability and electron-richness which is similar to tertiary phosphine ligands activating the oxidative addition step in the catalytic cycle of cross-coupling reactions.<sup>27–30</sup> As extension of NHC catalytic system, magnetic and silica-supported NHC heterogeneous catalysts were also reported.<sup>31–33</sup> Self-assemblies from poly(imidazole-palladium) and palladium N-heterocyclic carbene polymers were developed to achieve not only high recycling rate but also the highest TON

Department of Material and Life Chemistry, Faculty of Engineering, Kanagawa University, 3-27-1 Rokkakubashi, Kanagawa-ku, Yokohama, 221-8686, Japan.  
E-mail: kaikake@kanagawa-u.ac.jp; rhjin@kanagawa-u.ac.jp

† Electronic supplementary information (ESI) available. See DOI: 10.1039/d1ra06177a



and TOF.<sup>34–36</sup> Polystyrene-supported NHC–Pd(II) complex based on theophylline and a bis-NHC–palladium catalyst prepared from caffeine were reported as a good catalyst for coupling reactions.<sup>37,38</sup> However, compared to the great achievements of the homogeneous system of palladium catalysts, heterogeneous catalysis for C–C cross-coupling reaction has not generation update.

In our early study, we elucidated that xanthine derivatives, such as theophylline and theobromine, are strong ligands for selectively capturing palladium chloride even in the hydrochloric acid media to form complex comprised of two molecules of xanthine derivatives and a palladium chloride by chelate bond.<sup>39,40</sup> Focusing on the feature of strong coordination of theophylline to palladium(II), we have developed an excellent adsorbent of porous polystyrenic sub-5 micrometer spheres bearing theophylline residues and found that the adsorbent with trapping Pd(II) ions plays well as a catalyst in the Suzuki–Miyaura C–C coupling reaction in aqueous media.<sup>41</sup> This promoted us to explore theophylline-mediated heterogeneous palladium catalyst system. In this work, we found that complexation-driven self-assemblies between bis-theophylline alkane and PdCl<sub>2</sub> in aqueous media results in microflowers packed densely by nanopetals. The microflowers are insoluble in usual organic solvents and strong acidic medium but play as excellent heterogeneous catalyst in the Suzuki–Miyaura C–C coupling reaction with immortally recyclable feature.

## Experimental

### Materials

All compounds used in the synthesis and analysis were purchased from standard commercial suppliers and used as received without further purification.

### Synthesis of bis-theophylline heptane (BTC<sub>7</sub>)

To a 300 mL eggplant type flask equipped with a condenser, methanol (200 mL), K<sub>2</sub>CO<sub>3</sub> (25 mmol), theophylline (22 mmol), and dibromoheptane (10 mmol) were added the mixture was refluxed at 80 °C for 96 h. Afterward, the reaction mixture was evaporated, and then extracted the products from chloroform/water. The final white powders (BTC<sub>7</sub>) were obtained *via* recrystallization from ethyl acetate.

### Preparation of microflowers of palladium–theophylline complex (PdBTC<sub>7</sub>)

Ethanol solution of BTC<sub>7</sub> (5.0 mmol dm<sup>−3</sup>) and 1.0 mol dm<sup>−1</sup> hydrochloric acid solution containing 5.0 mmol dm<sup>−3</sup> palladium(II) chloride were mixed with equal volume (250/250 in mL) and the mixture was left at room temperature for 1 month until the formation of a lot of yellow precipitates. The yellow precipitates (PdBTC<sub>7</sub>) were recovered by filtration and washed by water and ethanol, and then dried at room temperature.

### Microflowers catalyzed C–C coupling reaction between phenylboronic acid and bromobenzene

The powders of PdBTC<sub>7</sub> (0.1 mol% Pd), 5 cm<sup>3</sup> of water/ethanol (1/1 in volume) were added to a screw top tube. Then, phenylboronic acid (0.6 mmol), potassium carbonate (1.0 mmol), 4-

bromobenzene (0.5 mmol) were added in order. The mixture was stirred at 20 °C. After 2 h, 20 cm<sup>3</sup> of distilled water was added and the organic fraction (biphenyl and unreacted 4-bromobenzene) extracted by CDCl<sub>3</sub> was subjected to NMR spectroscopy to estimate the yield (%).

### Characterizations

The solid-state UV-Vis spectra were recorded on a SHIMADZU UV-2600 with integral sphere equipment. The FT-IR spectra were recorded on a Jasco FT/IR-4600 spectrometer by diffusing the samples in KBr pellets. <sup>1</sup>H NMR and <sup>13</sup>C NMR spectra were recorded on a JEOL ECA 600 MHz spectrometer. <sup>13</sup>C cross polarization magic angle spinning (CP/MAS) NMR spectra were obtained using a JEOL ECX-400II spectrometer operated at 100.53 MHz. The amount of theophylline residues in the microspheres was estimated from the nitrogen content of the elemental analysis, recorded on a ELEMENTAR vario MICRO cube CHN Analyzer. The palladium content rate in the PdBTC<sub>7</sub> was measured on residual rate with a thermogravimetric analyzer SHIMADZU DTG-60H after calcination at a heating rate of 10 °C min<sup>−1</sup> from 40 to 800 °C. SEM observations were taken on a using a HITACHI SU-8010 scanning electron microscope at 1.5 kV after the samples were sputtered with Pt particles. EDX measurements were performed by SEM equipped with energy dispersive spectrometer. The TEM observation was performed on a JEOL JEM-2100 instrument with acceleration voltage of 200 kV. XPS spectra were recorded on a JEOL JPS 9010MC type spectrometer with an Mg Kα (1253.6 eV) source operating at a power of 100 W (10 kV, 10 mA) in a vacuum of at least 5 × 10<sup>−6</sup> Pa. The measured binding energies were adjusted to the C 1s hydrocarbon peak at 284.6 eV. The X-ray diffraction (XRD) patterns were collected on a Rigaku Ultima IV Protectus X-ray diffractometer with Cu Kα radiation (λ = 0.15418 nm).

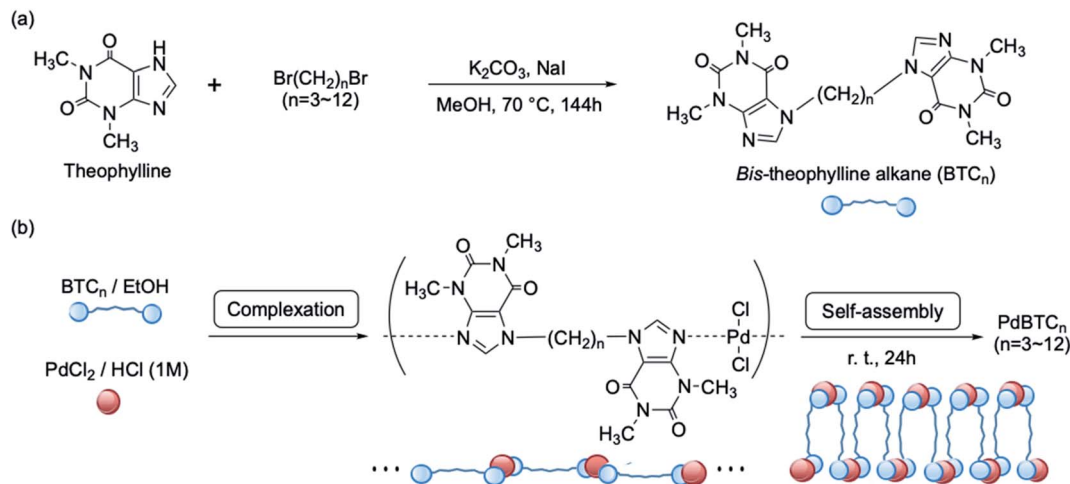
## Results and discussion

### Complexation-driven self-assembly from bis-theophylline alkane and PdCl<sub>2</sub>

Theophylline as a chelate type ligand has some advantages, for instance, strong ligand for selectively capturing palladium chloride, stable against air and moisture, enough hydrophilicity and low toxicity. Herein, we chose a very simple chemical process to link two theophylline residues with an alkyl chain, by which bis-theophylline alkanes (BTC<sub>n</sub>, *n* is carbon number in alkyl linker) with different alkyl length were produced (Scheme 1a). Our aim here is to trigger self-assembly of BTC<sub>n</sub> with Pd(II) in aqueous media because BTC<sub>n</sub> is capable of acting as amphiphile. As shown in Scheme 1b, mixing ethanol solution of BTC<sub>n</sub> (*n* = 3, 4, 5, 6, 7, 8, 9, 10, 11, 12) with PdCl<sub>2</sub> (in 1.0 M HCl) at room temperature for overnight (or more long time) yielded light yellow powders of Pd(II) complexes (PdBTC<sub>n</sub>). Unexpectedly, the powders once obtained could not be dissolved at all in polar and/or nonpolar solvents such as water, methanol, ethanol, DMF, DMSO, EtOAc, Et<sub>2</sub>O, CHCl<sub>3</sub>, *n*-hexane.

To access structural features of the PdBTC<sub>n</sub>, we chose powders of PdBTC<sub>7</sub> as a typical sample for the characterizations.





**Scheme 1** (a) Synthesis of bis-theophylline alkane (BTC<sub>n</sub>) as a ligand and (b) the preparation of Pd(II)-BTC<sub>n</sub> complex and the illustration of formation of self-assembled nanostructure palladium complexes (PdBTC<sub>n</sub>).

Firstly, we subjected the PdBTC<sub>7</sub> powders to SEM and TEM observation. As can be seen in Fig. 1a and b (SEM), the powders appeared as microspheres (in diameters 10–15 micrometer) with a lot of flower petals in their surface. From the magnified image, it is clear that the sphere is microflower in which a lot of nanopetals (ca. 15 nm in thickness) arrayed densely with radiation fashion toward outside. Similarly, the other PdBTC<sub>n</sub> complexes except PdBTC<sub>3</sub> were also globular aggregates assembled from nano-ribbons and nanosheets (see Fig. S17†). The EDX/SEM mapping images of PdBTC<sub>7</sub> indicate that both Pd (orange dots) and Cl (yellow dots) species are uniformly distributed through the spheres (Fig. 1d and e). We visualized a fragment of nanopetal by TEM. Apparently, a lot of dot-like nanoparticles about 20 nm in diameter were distributed through the petal (Fig. 1f). These nanoparticles would be assigned to Pd metallic nanoparticles which are probably generated under electron beam reduction during TEM measurement. To further confirm the state of palladium species, we performed XPS measurements. As seen in Fig. 1g, two peaks appeared at binding energy of 338.0 and 343.2 eV in the region of Pd 3d<sub>5/2</sub> and Pd 3d<sub>3/2</sub>, respectively, indicating the existence of cationic Pd(II) species. Elementary analysis and TG-DTA analysis (see Table S1†) also support the component of the powders of PdBTC<sub>7</sub> consisted of PdCl<sub>2</sub> and BTC<sub>7</sub> in 1 : 1 ratio. The content of carbon (39.53%) and nitrogen (17.78%) was well agreement with the calculated values of C (39.79%) and N (17.68%) in a form of {PdCl<sub>2</sub>/BTC<sub>7</sub>}. From TGA weight loss curve after heating to 800 °C, palladium content was estimated as 16.48% which is well agreement with the Pd value of 16.79% calculated from {PdCl<sub>2</sub>/BTC<sub>7</sub>}. Based on the above results, it is conclusive that PdBTC<sub>7</sub> is a polymeric complex with the repeat unit of (PdCl<sub>2</sub>-T(CH<sub>2</sub>)<sub>7</sub>T). To understand the features of chemical bonding of the polymeric complex, we further subjected the powders of PdBTC<sub>7</sub> to the measurements of UV-Vis, FT-IR and solid state <sup>13</sup>C NMR spectroscopies. Compared to the absorption of the theophylline derivative of BTC<sub>n</sub>, in the UV-Vis spectra, new absorption peaks appeared at 330 and 420 nm for PdBTC<sub>n</sub> (Fig. S13†) indicating the formation of coordination

bond of the theophylline residue to Pd(II) ion. Here, the two absorption bands appeared at longer wavelength should be assigned to exciton coupling of charge transfer in Pd-N bonds where the N atom is the electron donor and Pd is the electron acceptor.<sup>42</sup> In the FT-IR spectrum, the powders of PdBTC<sub>7</sub> showed characteristic bands at 3090 and 2927 cm<sup>-1</sup> corresponding to the C-H stretching vibrations of the alkyl linker and the C=O stretching vibrations at 1712, 1665 cm<sup>-1</sup> arisen from the theophylline residue (Fig. S14†). Compared with the bis-theophylline ligand BTC<sub>7</sub>, in the PdBTC<sub>7</sub> complex, the C-H stretching vibrations were shifted to the low wavenumber while C=O stretching vibrations were shifted to the high wavenumber. Also, in the solid state <sup>13</sup>C CP/MAS NMR spectra of PdBTC<sub>7</sub>, it was confirmed that the carbon signals at 150, 144, 140 and 105 ppm, which should be assigned to the xanthine group, were shifted to the lower magnetic field, while the signal at 46 ppm due to -NCH<sub>2</sub>- in alkyl linker was shifted to 44 ppm after complexation (Fig. S15†). Here, it is sure that because the nitrogen with lone pair electron on imidazole analogy binds to palladium by donating electron into an empty d-orbital of the palladium ion, the electron density on xanthine ring become lower and thus there appeared downfield shift of the above chemical shift. In the XPS spectra (Fig. S16†) of N 1s bonding energy, the ligand of BTC<sub>7</sub> showed two peaks assigned to C-N-C (399.8 eV) and C=N-C (398.2 eV). After formation of the complex of PdBTC<sub>7</sub>, the imine peak of C=N-C (398.2 eV) disappeared while peak due to C-N-C shifted slightly to 399.9 eV, indicating the formation of coordination bond between imine N and Pd(II).<sup>43</sup> As mentioned in the above SEM observation, the powders of PdBTC<sub>7</sub> are nanopetals-gathered flower-like microsphere self-assembled from PdCl<sub>2</sub> and BTC<sub>7</sub> (see Fig. 1a, b and S17†). Therefore, it is easily conceivable that the formation of nanopetals would be related to the hydrophobic interactions between the alkyl linkers within two theophylline moieties. With this in mind, we performed X-ray powder diffraction (XRD) measurement for the microflowers of PdBTC<sub>7</sub> (see Fig. 1h, S18 and S19†). The microflowers showed remarkable crystalline pattern with many diffraction peaks in the wide range of 2θ. Especially, the peak appeared at low angle of 8.70° (10.16 Å) would be





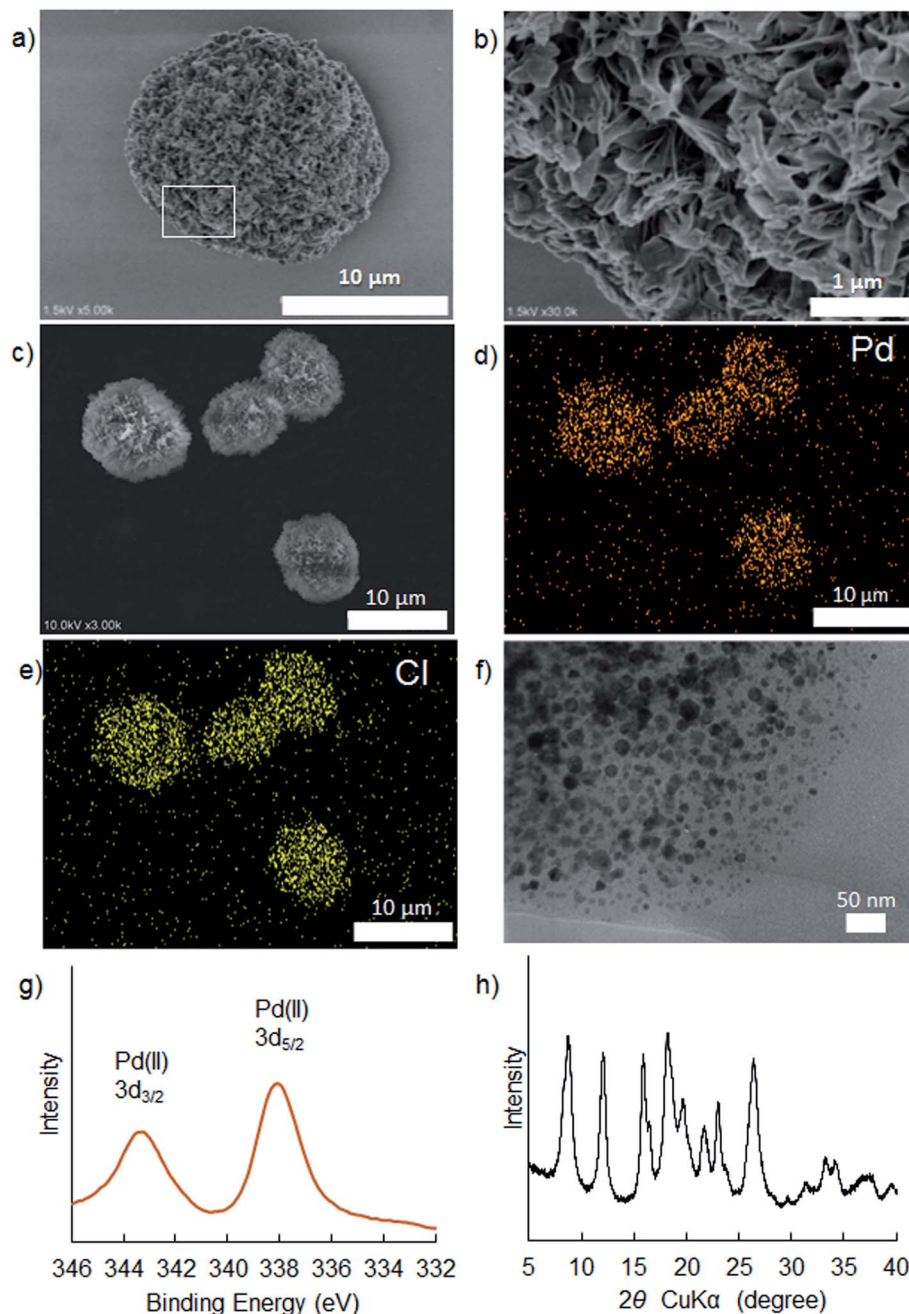


Fig. 1 Characterizations of microflower of PdBTc<sub>7</sub>: SEM image (a) and its magnification (b); EDX images of Pd (d) and Cl (e) in the SEM image of (c); TEM image (f); XPS (g) and XRD (h) spectra.

contributed to the period packing structure of heptane chain linked with two nitrogen atoms N(CH<sub>2</sub>)<sub>7</sub>N whose length just fits 10.10 Å. Undoubtedly, the polymerization *via* complexation between PdCl<sub>2</sub> (A<sub>2</sub> monomer) and BTC<sub>7</sub> (B<sub>2</sub> monomer) triggered the self-organization to give the microflowers.

#### Catalytic activity of the microflowers in C–C coupling reaction

From the above characterizations, we are sure that the complexes of PdBTc<sub>n</sub> would be good candidates of heterogeneous catalysts for C–C cross coupling reactions. So, we performed Suzuki–Miyaura coupling reaction between

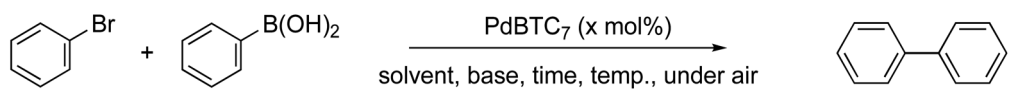
bromobenzene (BB) and phenylboronic acid (PBA) using the powders of PdBTc<sub>n</sub> as heterogeneous catalysts (Pd 0.1 mol% to bromobenzene) in water–ethanol at 20 °C. As summarized in Table S2,<sup>†</sup> all the complexes PdBTc<sub>n</sub> (*n* = 3–12) showed good catalytic activity to quantitatively yield biphenyl. Here, we especially focused our attention to the catalysis of PdBTc<sub>7</sub> due to its characteristic shape of microscale spherical flowers with nanopetals. In order to screen the optimum reaction conditions of the catalysis of the microflower of PdBTc<sub>7</sub>, we carried out the coupling reaction between BB and PBA by alteration of the kind of solvent, temperatures, times, catalytic amount and the kind of base. The details were summarized in Table 1. When the



coupling reaction was carried out using  $K_2CO_3$  as base in  $H_2O/EtOH$  (1 : 1) with 0.1 mol%  $PdBTC_7$  to BB at 20 °C and in air atmosphere for 2 hours (entry 1 in Table 1), biphenyl was produced in 98% yield. This clearly demonstrates that the microflowlers of  $PdBTC_7$  have high catalytic activity even under air condition. We found that the catalysis of the microflowlers strongly depended on the solvent (see entry 2–6 in Table 1). In water, the catalytic activity decreased remarkably, and in isopropanol or THF no reaction took place. The medium of water-ethanol (50/50 in volume) is better to give biphenyl quantitatively. It is known that compared to only using water, the mixture of water and alcohols is a good solvent for the  $Pd(II)$  precatalyzed C–C coupling reaction because alcohols could play as reducing agents to reduce  $Pd(II)$  precatalyst into  $Pd(0)$  clusters. Of course, primary alcohol is more active reducing agent than secondary one. In our case, the initial catalyst is not  $Pd$  nanoparticles but belongs to  $Pd(II)$  precatalyst. In this sense, we think that ethanol is better than isopropanol in the theophylline– $Pd(II)$  precatalyst system. Moreover, dissociation constant ( $pK_a$ ) of ethanol is smaller than that of isopropanol which is also benefit to the  $Pd(II)$ -based C–C coupling reaction because the catalytic cycle of hydrodehalogenation could be caused by primary alcohol.<sup>44</sup> Other conditions such as the kind of base, reaction time, and amount of catalyst also affect remarkably the yield of biphenyl product. In the mixture of water–ethanol in 50/50, base of  $K_2CO_3$  played as good additive than the others to make sure of the catalyst of the microflowlers activating the

reaction. Interestingly, even in the condition of reducing the catalyst amount from 1.0 mol% to 0.01 mol%, the reaction could yield 70% of biphenyl at 20 °C by 2 h indicating considerable catalytic activity of the microflowlers. Therefore, we performed the reaction by tuning simultaneously the conditions by reducing the catalyst amount and extending the reaction times. For instance, in the conditions of 0.001 mol%  $PdBTC_7/20$  °C/6 h, the yield of biphenyl reached 80%, which corresponds to TON of 80 000 and TOF of  $13\,300\ h^{-1}$ . Surprisingly, we found that in the presence of trace amount of  $PdBTC_7$  (0.0001 mol%), the value of TON increased extraordinarily to 320 000 by extending the reaction to 72 h. This means that the catalyst of  $PdBTC_7$  is extremely stable even under long reaction times. Feringa *et al.* reported that the presence of dissolved oxygen in water was crucial to speed up the reaction by generating an active form of the  $Pd$ -catalyst.<sup>45a</sup> Also, it is well demonstrated by Liu *et al.* that oxygen can effectively promote  $Pd(II)$ -precatalyst based Suzuki–Miyaura coupling reaction.<sup>45b</sup> The role of oxygen in the  $Pd$ -catalysis cycle is in capping  $Pd(0)$ -clusters which are very active species, but  $N_2$  could not cap  $Pd(0)$ -cluster. Thus  $O_2$  could efficiently suppress the fusion of  $Pd(0)$ -clusters and prevent the formation of  $Pd(0)$ -nanoparticles in catalysis cycle. Liu's work revealed that the  $Pd(0)$ -nanoparticles larger than 1.5 nm formed from  $Pd(II)$ -precatalyst deteriorate greatly catalytic activity. Exactly, in our case, the reaction retarded evidently under nitrogen flow yielding biphenyl only in 39% at 20 °C for 2 h which is largely lower than 98% yield in air condition

Table 1 Optimization of reaction conditions for the coupling of bromobenzene with phenylboronic acid, catalyzed by  $PdBTC_7$ <sup>a</sup>

								
Entry	Solvent <sup>b</sup>	T [°C]	Time [h]	$PdBTC_7$ [mol%]	Base	Yield <sup>c</sup> [%]	TON	TOF [ $h^{-1}$ ]
1	$H_2O$ –ethanol	20	2	0.1	$K_2CO_3$	98	980	490
2	$H_2O$	20	2	0.1	$K_2CO_3$	8	80	40
3	$H_2O$	50	24	0.1	$K_2CO_3$	98	980	20
4	Ethanol	20	2	0.1	$K_2CO_3$	97	970	485
5	Iso-propanol	20	2	0.1	$K_2CO_3$	0	0	0
6	THF	20	2	0.1	$K_2CO_3$	0	0	0
7	$H_2O$ –ethanol	20	2	0.1	NaOH	97	970	485
8	$H_2O$ –ethanol	20	2	0.1	$K_3PO_4$	58	580	290
9	$H_2O$ –ethanol	20	2	0.1	$Et_3N$	9	90	45
10	$H_2O$ –ethanol	20	0.5	1.0	$K_2CO_3$	93	93	186
11	$H_2O$ –ethanol	20	0.5	0.1	$K_2CO_3$	54	540	1080
12	$H_2O$ –ethanol	20	0.5	0.01	$K_2CO_3$	15	1500	3000
13	$H_2O$ –ethanol	20	1	1.0	$K_2CO_3$	98	98	98
14	$H_2O$ –ethanol	20	1	0.1	$K_2CO_3$	95	950	950
15	$H_2O$ –ethanol	20	1	0.01	$K_2CO_3$	41	4100	4100
16	$H_2O$ –ethanol	20	2	1.0	$K_2CO_3$	98	98	49
17	$H_2O$ –ethanol	20	2	0.01	$K_2CO_3$	70	7000	3500
18	$H_2O$ –ethanol	20	6	0.001	$K_2CO_3$	80	80 000	13 333
19	$H_2O$ –ethanol	20	72	0.0001	$K_2CO_3$	32	320 000	4444
20	$H_2O$ –ethanol	20	2	0.1 (under $N_2$ )	$K_2CO_3$	39	390	195
21	$H_2O$ –ethanol	50	2	0.1	$K_2CO_3$	100	1000	500

<sup>a</sup> Reaction conditions: aryl halides (0.5 mmol), phenylboronic acid (0.6 mmol), base (1.0 mmol), solvent (5.0 mL). <sup>b</sup>  $H_2O$  : ethanol = 1 : 1. <sup>c</sup> Yields were determined by  $^1H$ -NMR analysis.



(Table 1, entry 20). This is well agreement with the Liu's proposed mechanism of oxygen promoted Pd(II)-precatalyst based catalysis cycle. It needs to note here that the microflowers with nanopetals of theophylline-Pd complexes once formed are not soluble in any solvents. For comparison, we examined two kinds of catalysts (one is a water-soluble polymers bearing theophylline-Pd complex (not published) and other one is heterogeneous theophylline-Pd(II) catalyst supported by polystyrenic spheres<sup>41</sup>) in C-C coupling reaction between BB and PBA in the same conditions, but no predominance in the yields of biphenyl appeared than the case of microflowers. It is conceivable that the nanopetals on microflowers, which have a lot of Pd species in their surface, might be helpful in concentration and diffusion of the substances and thus promote the reaction. Therefore, we consider that the microflowers self-organized from the complexation of Pd(II) and theophyllines have advantage as heterogeneous catalysts.

Based on the above results, we further performed the C-C coupling reactions using a series of derivatives of aryl bromides with substituents of -CH<sub>3</sub>, -OMe, -OH, -NH<sub>2</sub>, -CHO, -COOH, -CN, -NO<sub>2</sub>, -C(=O)Me in *ortho*-, *meta*- and *para*-positions. The details were summarized in Table 2. Interestingly, *p*-substituted aryl bromides regardless of the type of substituents of electron donating or electron withdrawing group (except -NH<sub>2</sub>) showed high reactivity giving products in over 90% yield by 6 h. In case of *ortho*- and *meta*-substituent, the aryl bromides with the groups of -CH<sub>3</sub>, -OMe, -OH and -COOH also showed high reactivity. However, the reactivity decreased as the substituent in *ortho*- and *meta*-position was replaced by the electron withdrawing groups such as -CHO, -CN, -NO<sub>2</sub>, -C(=O)Me, and no reaction took place in case of the substituents of *ortho*-NO<sub>2</sub> and -C(=O)Me. It is sure that the ligand of theophylline in Pd complex is a larger planar ring with  $\pi$  electric dipole. In the aqueous medium, this planer ligand would interact with the

aryl bromide by  $\pi$ - $\pi$  interactions and thus assists the insertion of Pd to the Ar-Br bond in the step of oxidative addition. Probably, in this step, the position and kinds of substituents on bromobenzene affect the approaching of aryl bromide to the active center of theophylline-Pd(0)-theophylline. The substituents of electron withdrawing in *ortho*- or *meta*-positions perhaps hinder geometrically and electronically the interactions between theophylline moieties and aryl bromide, and thus raises barrier of the oxidative addition (but further investigation is needed for clearing the reason).

### Recyclable microflowers catalyst in C-C coupling reaction

In the heterogeneous catalysis system, the most important issue is to recycle the catalyst without deactivation and leaching. To confirm the recyclability of the microflowers of PdBTC<sub>7</sub>, we performed ten times of reusing test of the microflowers recovered by quickly filtering each time of reaction mixture through membrane filter. As shown in Fig. S20,<sup>†</sup> almost quantitative yield (>95%) of biphenyl was produced in 7 times of reusing the microflowers. Afterward, however, the yields decreased remarkably from 8 recycles step by step and were down to below 10% as repeating 10 recycles, indicating the severe loss of catalytic activity of the PdBTC<sub>7</sub>. We observed that the color of the powders of PdBTC<sub>7</sub> was blackish green until the 5 times of reusing but changed to black step by step. To understand the reason of the deactivation, we subjected the recovered powders of PdBTC<sub>7</sub> after 10 recycles to SEM and XPS measurements. As shown in SEM images (Fig. 2a-c and S21<sup>†</sup>), the early globular morphology with flower-like surface was almost broken to fragments after reusing 6 times. Further reuse caused the flocculation of the broken fragments and finally resulted in larger irregular particles with smooth surface after ten recycles. With deformation of the morphology, chemical changes also

Table 2 Effect of substituents in *ortho*-, *meta*- and *para*-position on the coupling reactions catalyzed by PdBTC<sub>7</sub><sup>a</sup>

Substituent (R <sub>1</sub> )	Conversion <sup>b</sup> [%]			TON			TOF [h <sup>-1</sup> ]		
	-o	-m	-p	-o	-m	-p	-o	-m	-p
	2 h/6 h	2 h/6 h	2 h/6 h	2 h/6 h	2 h/6 h	2 h/6 h	2 h/6 h	2 h/6 h	2 h/6 h
-CH <sub>3</sub>	56/94	86/87	98/99	560/940	860/870	980/990	280/157	430/145	490/165
-OCH <sub>3</sub>	72/94	33/96	45/99	720/940	330/960	450/990	360/157	225/160	225/165
-OH	58/71	73/92	67/93	580/710	730/920	670/930	290/118	365/153	335/155
-NH <sub>2</sub>	3/8	46/81	32/63	30/80	320/630	320/630	15/13	160/105	160/105
-CHO	21/94	99/100	94/96	210/940	990/1000	940/960	105/157	495/167	470/160
-COOH	62/74	79/92	66/93	620/740	790/920	660/930	310/123	395/153	330/105
-CN	31/34	68/68	98/99	310/340	680/680	980/990	155/57	340/113	490/165
-NO <sub>2</sub>	0/0	17/36	44/99	0/0	170/360	440/990	0/0	85/60	220/165
-COCH <sub>3</sub>	0/0	1/6	67/97	0/0	10/60	670/970	0/0	5/10	335/162

<sup>a</sup> Reaction conditions: aryl halides (0.5 mmol), phenylboronic acid (0.6 mmol), base (1.0 mmol), solvent (5.0 mL). <sup>b</sup> Yields at 2 h and 6 h reactions were determined by <sup>1</sup>H-NMR analysis.



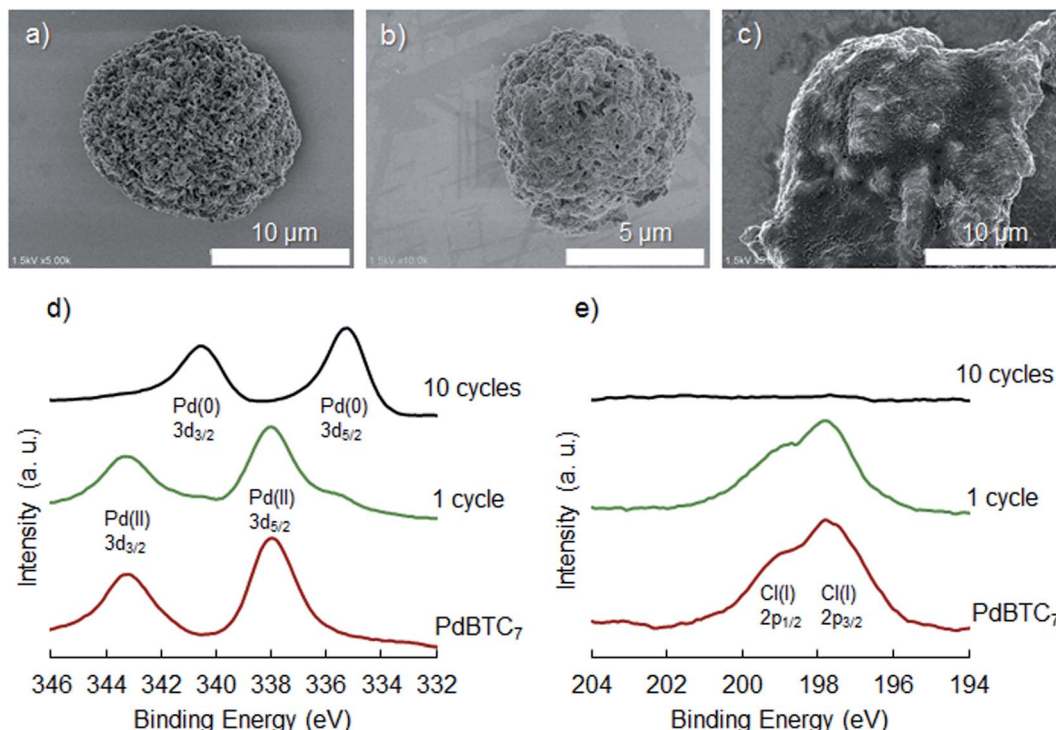


Fig. 2 Evaluation of catalysts on recycling experiments. (a) SEM image of intact PdBTC<sub>7</sub>, (b) PdBTC<sub>7</sub> after first reaction, (c) PdBTC<sub>7</sub> after ten cycles reactions, and (d) comparison of XPS narrow scan for Pd 3d, (e) XPS narrow scan for Cl 2p.

accompanied in the Pd catalytic center. Fig. 2d and e show XPS spectra of the catalysts as intact and after using 1 and 10 times. By comparison with the case of the intact microflowers, we can see that two peaks due to Pd<sup>2+</sup> cation bonding energies at 340.6 and 338.0 eV vanished for the powders after ten recycles. Instead, two new peaks appeared at lower binding energies at 340.6 and 335.3 eV, which should be attributed to the species of palladium metal corresponding to Pd(0)3d<sub>3/2</sub> and Pd(0)3d<sub>5/2</sub> spin orbit splitting.<sup>46,47</sup> In addition, the peaks due to Cl<sup>-</sup> anion in the range of 196–200 eV also completely disappeared after ten recycles. This result reveals unambiguously that after ten times of recycle, the Pd<sup>2+</sup> cation was completely converted to Pd<sup>0</sup> metal accompanying loss of Cl<sup>-</sup> counter anion, which would be a reason of the loss of catalytic activity of the PdBTC<sub>7</sub>. Therefore, we think that the essential issue of increasing recycling

performance of the PdBTC<sub>7</sub> microflowers is to keep divalent Pd(II) species without loss of Cl<sup>-</sup> ion in the reaction running.

With this in mind, firstly, we investigated the effect of NaCl additive by changing its amount from 0 to 5.0-fold equivalent to bromobenzene in the presence of 0.1 mol% PdBTC<sub>7</sub>. It was found that the amount of NaCl below 2-fold equivalent, the coupling reaction proceeded quantitatively (see Table S3†). However, when the amount of NaCl was largely over 2-fold equivalent to bromobenzene, the yield of biphenyl decreased. This indicates that large excess of NaCl is not promise. Based on this screening, we performed 20 times of reusing the microflowers in the reaction between BB and PBA by setting the amount of NaCl (0.5 mmol) in every recycle. Surprisingly, the yield of biphenyl retained up 95% until the 19th-recycle and slightly decreased to 87% in the 20th-recycle (see Fig. 3). On the

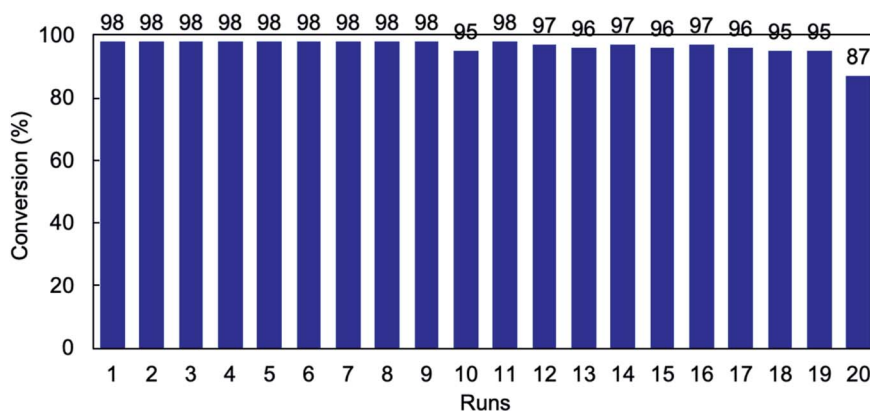


Fig. 3 Recyclability tests of PdBTC<sub>7</sub> for the coupling reaction of bromobenzene and phenylboronic acid under chloride ion (0.5 mmol).



other hand, the globular morphology with flower-like surface remained even after 20-recycles (see SEM images in Fig. S22†). This is as if the catalyst of the PdBTC<sub>7</sub> microflowers becomes immortal for the cross-coupling reaction in the presence of NaCl.

To answer the reason why there is no deactivation until 20 times recycles, we subjected the powders recovered after 10th- and 20th-recycle to XPS measurement. As shown in XPS spectra (see Fig. 4), compared to the original sample, the catalyst reused after 10- and 20-recycles preserved still the peaks arisen from Pd<sup>2+</sup> cation following small peaks due to Pd<sup>0</sup> species. In addition, the peaks due to Cl<sup>−</sup> anion also remained. The interest here is why NaCl can assure the catalytic activity of the microflowers in recycle. It is widely known that in the Suzuki–Miyaura cross-coupling reaction, the precatalyst of Pd(II) ion before entering the catalytic cycle must be reduced into Pd<sup>0</sup> which is promoted by base additives such as K<sub>2</sub>CO<sub>3</sub>, Ca(OH)<sub>2</sub>, NaOH and organic amines. Afterward, the complex of Pd<sup>0</sup> activates aryl halide (Ar<sup>1</sup>–X) *via* oxidative addition to form Ar<sup>1</sup>–Pd(II)–X which causes transmetalation with arylboronic acid (Ar<sup>2</sup>B(OH)<sub>2</sub>) to give Ar<sup>1</sup>–Pd(II)–Ar<sup>2</sup> that follows reductive elimination to yield Ar<sup>1</sup>–Ar<sup>2</sup> coupling product while palladium comes back to Pd<sup>0</sup>. In this cycle, one of the reasons of deactivation of the catalyst should be the aggregation or fusion of the complexed Pd<sup>0</sup>, which results in larger metallic Pd. From the TEM images as shown in Fig. S23,† we can see that the dot-like palladium

nanoparticles were retained even after using 10 and 20 times in the presence of NaCl although there are slight changes compared to the intact form of the microflowers with a lot of nano-dot (note: the nano-dots were formed due to electron beam reduction of Pd(II) during TEM measurement). In contrast, from the sample of reusing 10 times without NaCl, only large dark aggregates without any trace of nano-dots were observed. Therefore, in our system of the PdBTC<sub>7</sub> microflowers, it is important to block the fusion from the small cluster of Pd<sup>0</sup>-trapped by theophylline residues into metallic Pd or to prevent the destruction and/or the deformation of the catalyst morphology from microflowers to irregular sediments. The results of XPS, SEM and TEM of the catalyst after 20-recycle test in the presence of NaCl additive clearly indicate that there is not formation of metallic Pd aggregates and destruction of the globular morphology. We think that in the PdBTC<sub>7</sub> microflowers, not all the Pd(II) participate the catalytic cycle; a part of Pd(II) cations trapped inside nanopetals should be employed to support the nanopetals architecture for maintaining toughness. Only the Pd(II) cations, which are located on the surface of the nanopetals, act as true precatalyst. Therefore, Cl<sup>−</sup> ion is indispensable ingredient. The role of the additive NaCl here would be to stabilize the morphology of microflowers *via* interaction with Pd(II). Once the morphology remained without destruction, the palladium species coordinated by theophylline moieties can keep the catalytic activity because there is no leaching (see the

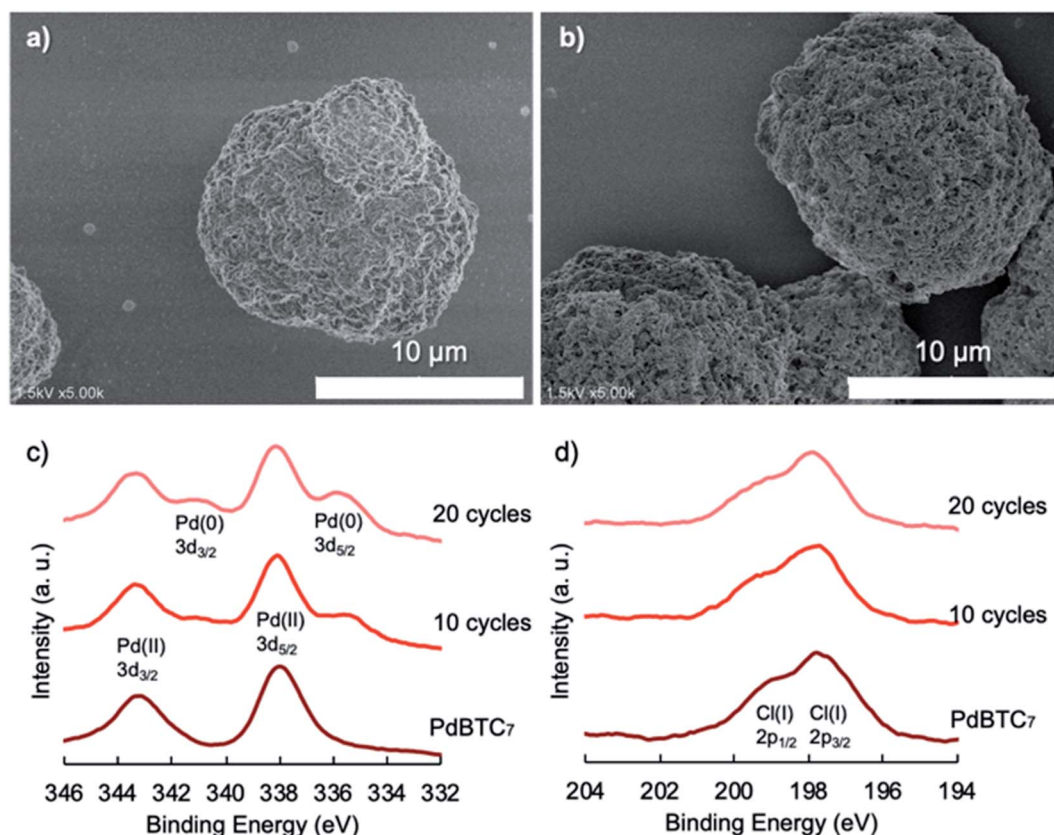


Fig. 4 Influences of NaCl additive on the structures of catalyst reused. (a) SEM images of PdBTC<sub>7</sub> after 10th cycles coupling reactions, (b) after 20th cycles reactions and (c) comparison of Pd element in XPS, (d) comparison of Cl element in XPS.





hot filtrate test in ESI<sup>+</sup>) and/or fusion of palladium during the reaction. Consequently, our Pd(II)-precatalyst of the microflowers exhibit unusual immortal feature even if the recycle was carried out 20 times. There are some reports demonstrating that the addition of chloride ion can chelate palladium to maintain a small angle of ligand to Pd (P–Pd–P) and thus lower the activation barrier of the oxidative addition in the cross-coupling catalytic cycle.<sup>48,49</sup> We found that too excess of NaCl is not good in the yield of biphenyl. So, we speculate that besides the roles of Cl<sup>−</sup> ion mentioned above, a suitable amount of chloride ion may be also helpful for reducing the reaction barrier on the oxidative addition.<sup>50</sup> This is still a question to be searched in the future.

## Conclusions

In this work, we demonstrated that NaCl is a key additive to enhance the recyclability of the PdBTC<sub>7</sub> microflowers with high catalytic activity. Although there are many reports focusing the catalysis of palladium supported by the organics and inorganics in the cross-couplings, no example, as far as we know, showed so successful recyclability as seen in PdBTC<sub>7</sub> microflowers. Theophylline is a chemically and thermochemically stable compound. We have clarified in our early work that the complexes formed by Pd(II) and theophyllines are stable in the strong acids such as HCl, HNO<sub>3</sub> and H<sub>2</sub>SO<sub>4</sub>. The decomplexation occurs in the limited conditions such as in the high concentrations of ammonia and/or thiourea solutions.<sup>39–41</sup> Therefore, we believe that Pd(II)–theophyllines microflowers produced *via* complexation-driven self-assembly have great potential for developing generation-updated heterogeneous catalyst for the C–C cross coupling. Further related study using Pd(II)–theophylline-based heterogeneous catalysts is in progress.

## Conflicts of interest

There are no conflicts to declare.

## Acknowledgements

This work was partly supported by JSPS KAKENHI grant number JP19K05571.

## References

- 1 N. Miyaura, T. Yanagi and A. Suzuki, *Synth. Commun.*, 1981, **11**(7), 513–519.
- 2 C. Torborga and M. Beller, *Adv. Synth. Catal.*, 2009, **351**, 3027–3043.
- 3 (a) H. Nakanotani, T. Higuchi, T. Furukawa, K. Masui, K. Morimoto, M. Numata, H. Tanaka, Y. Sagara, T. Yasuda and C. Adachi, *Nat. Commun.*, 2014, **5**, 4016; (b) H. Nakanotani, Y. Tsuchiya and C. Adachi, *Chem. Lett.*, 2021, **50**, 938–948.
- 4 H. Sasabe and J. Kido, *J. Mater. Chem. C*, 2013, **1**, 1699–1707.
- 5 M. Shimizu, I. Nagao, Y. Tomioka and T. Hiyama, *Angew. Chem., Int. Ed.*, 2008, **47**, 8096–8099.
- 6 C. J. Seechurn, M. O. Kitching, T. J. Colacot and V. Snieckus, *Angew. Chem., Int. Ed.*, 2012, **51**, 5062–5085.
- 7 W. A. Herrmann, C. Brossmer, K. Öfele, C. P. Reisinger, T. Priermeier, M. Beller and H. Fischer, *Angew. Chem., Int. Ed.*, 1995, **34**, 1844–1848.
- 8 W. A. Herrmann, C. Brossmer, C. P. Reisinger, T. H. Riermeier, K. Öfele and M. Beller, *J. Eur. Chem.*, 1997, **3**, 1357–1362.
- 9 M. R. Biscoe, B. P. Fors and S. L. Buchwald, *J. Am. Chem. Soc.*, 2008, **130**, 6686–6687.
- 10 T. Kinzel, Y. Zhang and S. L. Buchwald, *J. Am. Chem. Soc.*, 2010, **132**, 14073–14075.
- 11 N. C. Bruno and S. L. Buchwald, *Org. Lett.*, 2013, **15**, 2876–2879.
- 12 N. C. Bruno, N. Niljianskul and S. L. Buchwald, *J. Org. Chem.*, 2014, **79**, 4161–4166.
- 13 M. Pagliaro, V. Pandarus, R. Ciriminna, F. Béland and P. D. Cará, *ChemCatChem*, 2012, **4**, 432–445.
- 14 L. Yin and J. Liebscher, *Chem. Rev.*, 2007, **107**, 133–173.
- 15 A. Biffis, P. Centomo, A. D. Zotto and M. Zecca, *Chem. Rev.*, 2018, **118**, 2249–2295.
- 16 A. Balanta, C. Godard and C. Claver, *Chem. Soc. Rev.*, 2011, **40**, 4973–4985.
- 17 A. Fihri, M. Bouhrara, B. Nekoueishahraki, J.-M. Basset and V. Polshettiwar, *Chem. Soc. Rev.*, 2011, **40**, 5181–5203.
- 18 A. J. Reay and I. J. S. Fairlamb, *Chem. Commun.*, 2015, **51**, 16289–16307.
- 19 M. Gholinejad, Z. Naghshbandi and C. Nájera, *ChemCatChem*, 2019, **11**, 1792–1823.
- 20 A. W. Augustyniak, W. Zawartka, J. A. R. Navarro and A. M. Trzeciak, *Dalton Trans.*, 2016, **45**, 13525.
- 21 M. P. Lorenzo, *J. Phys. Chem. Lett.*, 2012, **3**, 167–174.
- 22 P. J. Ellis, I. J. S. Fairlamb, S. F. J. Hackett, K. Wilson and A. F. Lee, *Angew. Chem., Int. Ed.*, 2010, **49**, 1820–1824.
- 23 Y. Li, E. Boone and M. A. El-Sayed, *Langmuir*, 2002, **18**, 4921–4925.
- 24 L.-X. You, L.-X. Cui, B.-B. Zhao, G. Xiong, F. Ding, B.-Y. Ren, Z.-L. Shi, I. Dragutan, V. Dragutan and Y.-G. Sun, *Dalton Trans.*, 2018, **47**, 8755–8763.
- 25 V. Pascanu, Q. Yao, A. B. Gómez, M. Gustafsson, Y. Yun, W. Wan, L. Samain, X. Zou and B. M. Matute, *Chem.–Eur. J.*, 2013, **19**, 17483–17493.
- 26 (a) L. You, W. Zhu, S. Wanga, G. Xiong, F. Ding, B. Ren, I. Dragutan, V. Dragutan and Y. Sun, *Polyhedron*, 2016, **115**, 47–53; (b) L. You, S. Yao, B. Zhao, G. Xiong, I. Dragutan, V. Dragutan, X. Liu, F. Ding and Y. Sun, *Dalton Trans.*, 2020, **49**, 6368–6376; (c) L. You, B. Zhao, S. Yao, G. Xiong, I. Dragutan, V. Dragutan, F. Ding and Y. Sun, *J. Catal.*, 2020, **392**, 80–87; (d) L. You, W. Zong, G. Xiong, F. Ding, S. Wang, B. Ren, I. Dragutan, V. Dragutan and Y. Sun, *Appl. Catal., A*, 2016, **511**, 1–10.
- 27 G. C. Fortman and S. P. Nolan, *Chem. Soc. Rev.*, 2011, **40**, 5151–5169.
- 28 W. A. Herrmann and C. Köcher, *Angew. Chem., Int. Ed. Engl.*, 1997, **36**, 2162–2187.

- 29 M. Charbonneau, G. Addoumieh, P. Oguadinma and A. R. Schmitzer, *Organometallics*, 2014, **33**, 6544–6549.
- 30 M.-T. Chen and Z.-L. Kao, *Dalton Trans.*, 2017, **46**, 16394–16398.
- 31 V. Kandathil, B. D. Fahlman, B. S. Sasidhar, S. A. Patil and S. A. Patil, *New J. Chem.*, 2017, **41**, 9531–9545.
- 32 Z. Wang, Y. Yu, Y. X. Zhang, S. Z. Li, H. Qian and Z. Y. Lin, *Green Chem.*, 2015, **17**, 413–420.
- 33 T. Begum, M. Mondal, M. P. Borpuzari, R. Kar, G. Kalita, P. K. Gogoi and U. Bora, *Dalton Trans.*, 2017, **46**, 539–546.
- 34 H. Zhao, L. Li, Y. Wang and R. Wang, *Sci. Rep.*, 2015, **4**, 1–7.
- 35 S. M. Sarkar, Y. Uozumi and Y. M. A. Yamada, *Angew. Chem., Int. Ed.*, 2011, **50**, 9437–9441.
- 36 Y. M. A. Yamada, S. M. Sarkar and Y. Uozumi, *J. Am. Chem. Soc.*, 2012, **134**, 3190–3198.
- 37 F.-T. Luo and H.-K. Lo, *J. Organomet. Chem.*, 2011, **696**, 1262–1265.
- 38 E. Mohammadi and B. Movassagh, *J. Organomet. Chem.*, 2016, **822**, 62–66.
- 39 K. Kaikake and Y. Baba, *Anal. Sci.*, 2001, **17**, 411–415.
- 40 K. Kaikake and Y. Baba, *Solvent Extr. Ion Exch.*, 2002, **20**, 491–503.
- 41 K. Kaikake, M. Takada, D. Soma and R.-H. Jin, *RSC Adv.*, 2018, **8**, 34505–34513.
- 42 J. Dutta, M. G. Richmond and S. Bhattacharya, *Dalton Trans.*, 2015, **44**, 13615–13632.
- 43 A. Mohtasebi, T. Chowdhury, L. H. H. Hsu, M. C. Biesinger and P. Kruse, *J. Phys. Chem. C*, 2016, **120**, 29248–29263.
- 44 (a) J. Moon and S. Lee, *J. Organomet. Chem.*, 2009, **694**, 473–477; (b) Z. Ahmadi and J. S. McIndoe, *Chem. Commun.*, 2013, **49**, 11488–11490.
- 45 (a) D. Heijnen, F. Tosi, C. Vila, M. C. A. Stuart, P. H. Elsinga, W. Szymanski and B. L. Feringa, *Angew. Chem., Int. Ed.*, 2017, **56**, 3354–3359; (b) C. Liu and X. Li, *Chem. Rec.*, 2016, **16**, 84–97.
- 46 M. L. Kantam, M. Roy, S. Roy, B. Sreedhar, S. S. Madhavendra, B. M. Choudary and R. L. De, *Tetrahedron*, 2007, **63**, 8002–8009.
- 47 S. MacQuarrie, J. H. Horton, J. Barnes, K. McEleney, H.-P. Looock and C. M. Crudden, *Angew. Chem., Int. Ed.*, 2008, **47**, 3279–3282.
- 48 S. Kozuch, C. Amatore, A. Jutand and S. Shaik, *Organometallics*, 2005, **24**, 2319–2330.
- 49 C. Amatore and A. Jutand, *Acc. Chem. Res.*, 2000, **33**, 314–321.
- 50 T. Sengupta, D. Bista and S. N. Khanna, *ACS Catal.*, 2021, **11**, 11459–11468.

